Influence of Laser Pulse Energy on CFTS Thin Film Deposited by Pulsed Laser Deposition

Iman Rahmani and Majid Ghanaatshoar*

Laser and Plasma Research Institute, Shahid Beheshti University, Tehran, Iran

***Corresponding author email:** m-ghanaat@sbu.ac.ir

Regular paper: Received: Sep. 04, 2022, Revised: Jan. 09, 2023, Accepted: Jan. 13, 2023, Available Online: Jan. 15, 2023, DOI: 10.52547/ijop.16.2.131

ABSTRACT— We investigate the Cu_2FeSnS_4 (CFTS) thin film. The raw materials of this thin film are copper, iron and tin, which are mixed in the form of tablets and then are deposited on a glass substrate through the process of pulsed laser deposition (PLD). The produced metallic thin films are then sulfurized to carry out the process of merging the element sulfur in the thin films and forming CFTS structure. We investigate the influence of sulfurization temperature and the laser pulse energy in the PLD process on the deposited CFTS thin films. The X-ray diffraction (XRD), Raman and UV-Vis analyses' results show that by decrease in sulfurization temperature from 600 °C to 550 °C the crystal quality of the thin films is improved, which is realized by increase in volume and quality of the CFTS phase. On the other hand, the results confirm that the laser fluence is a decisive factor which should be taken into account to achieve an optimized structure.

KEYWORDS: Cu_2FeSnS_4 (CFTS), Thin Film, Pulsed Laser Deposition (PLD), Sulfurization.

I. INTRODUCTION

Solar cells convert solar energy into electricity. They are divided into three categories: cells based on crystalline silicon (first generation), cells based on thin films (second generation), and those based on organic materials and nanostructures (third generation). Among the second generation cells, the use of quaternary chalcogenides such as $Cu(In_xGa_{1-x})Se_2$ (CIGS) as the absorber layer of solar cells has led to satisfactory efficiency [1, 2], however it contains rare and toxic elements such as gallium and indium, which makes the application of this compound challenging. This idea draws researchers' attention to the use of other quaternary chalcogenides with the general formula Cu_2-M-IV-VI_4, as the absorber layer of the second generation solar cells. In this formula, M represents elements such as Fe, Zn and In, IV stands for the elements Sn and Ga, and VI symbolizes Se and S.

Cu_2ZnSnS_4 (CZTS) is the first candidate for replacement, but the formation of stable secondary phases makes its application a challenging task. Actually, the secondary phases such as SnS_2, Cu_2SnS_3, ZnS, and SnS_2 suppress the performance of the device by acting as defects and recombination centers, and by degrading the energy gap. Subsequently, efforts have been made to increase the efficiency of solar cells based on quaternary chalcogenide $Cu_2ZnSn(S_xSe_{1-x})$ by altering the S/Se ratio to get the optimum band gap and appropriate film microstructure. Precise control of the S/Se ratio is very difficult during the thermal annealing process. Therefore, some researchers decided to solve its limitations by changing some elements in CZTS [3]. Replacing elements such as Fe instead of Zn in CZTS composition creates almost the same energy gap, absorption coefficient and transport properties since their structures are closely related except for different space groups because of the difference in distribution of cations Zn^{2+} and Fe^{2+}. There are also reports that show this replacement can improve the optical and structural properties of the compound [4].

[Downloaded from mail.ijop.ir on 2026-11-26]

The elements in Cu_2FeSnS_4 (CFTS) are more abundant along with being non-toxic. The CFTS composition has a suitable bandgap (1.2-1.8 eV) and a high absorption coefficient (10^4 cm^{-1}), which make it appropriate as an absorber layer in solar cells. In a general classification, CFTS growth methods are divided into physical (such as sputtering, pulsed laser deposition (PLD), etc.) and chemical (such as spray pyrolysis, successive ionic layer adsorption and reaction (SILAR), spin coating, chemical bath deposition, etc.) methods, which include both vacuum and non-vacuum conditions. Vanalakar *et al*. carried out a relatively thorough review research in this field. They reviewed the synthesis, characterization and the barriers to achieve high efficiency in CFTS-based solar cells [5]. Although the research done on CFTS material is limited, but irrespective of physical and chemical techniques in the fabrication of CFTS thin films, the obtained results show that the post-annealing is a very important step to overcome defects and non-homogeneity of the thin films. The post-annealing improves the crystal quality and grain growth, and ultimately results in higher power conversion efficiency.

In this paper, we firstly deposit a mixture of copper, iron and tin with a ratio of 2:1:1 on a glass substrate by PLD method. PLD is a well-known method in terms of simplicity in machine design and reliable transfer of elements from the target to deposited film on the substrate [6, 7]. Then, we add the sulfur element to it by the sulfurization process to form the CFTS phase on the glass substrate. We examine the influence of the sulfurization temperature and subsequently the laser pulse energy on the properties of the deposited thin films. In this way, we try to find an optimum sulfurization temperature and the best value of the laser pulse energy during the PLD process.

II. EXPERIMENTAL METHOD

To produce the CFTS thin film, we first prepare the CFT tablet, which is used as the target material in the PLD process. For this purpose, Cu, Fe and Sn powders are mixed together by planetary mill method with molar ratios of 2:1:1 and the resulting mixture is turned into the tablets. We use the glass slide as substrate, which is very important to be cleaned to prevent impurities and resulting problems.

For deposition, we use the second harmonic of the Nd:YAG laser (λ=532 nm) with a pulse width of 8.5 nanoseconds and at a repetition rate of 10 Hz. The spot size on the target material is about 1.58 cm^2 with three different fluences of 3.82 J/cm^2, 4.58 J/cm^2 and 9.54 J/cm^2. We set the air pressure in the depositing process to 10^{-4} mbar and the distance from the substrate to the target to about 50 mm. Due to the fact that in the PLD process the target material must be uniformly hit by the laser beam, we use a 60-rpm motor to rotate the target material. Then we perform the PLD process of CFT material with the mentioned conditions for 20 minutes. Afterwards, we place the formed thin film of CFT in a sulfurization furnace for 20 minutes at a pressure of 4×10^{-2} mbar to convert it to CFTS. We do this at 550 °C and 600 °C temperatures. Finally, to characterize the grown CFTS thin film, we examine the X-ray diffraction (XRD) patterns, Raman spectra, and UV-Vis-IR results.

III. MATHEMATICS

The d-spacing (d_{hkl}), crystallite size (D), micro strain (ε) and the dislocation (δ) of the crystal structure of a thin film are obtained from the following equations [8]:

$$d_{hkl} = \frac{\lambda}{2\sin(\theta_{hkl})} \quad (1)$$

$$D = \frac{K\lambda}{\beta_{hkl}\cos(\theta_{hkl})} \quad (2)$$

$$\varepsilon = \frac{\beta_{hkl}\cos(\theta_{hkl})}{4} \quad (3)$$

$$\delta = \frac{1}{D^2} \quad (4)$$

θ_{hkl} is the X-ray diffraction angle, β_{hkl} equals to the width at half the maximum value (FWHM) of the index peak observed in the XRD pattern, constant K is 0.9, and λ is wavelength of the X-ray (1.54060 Å).

[Downloaded from mail.ijop.ir on 2026-11-26]

IV. Results and Discussion

Figure 1 shows the XRD patterns for samples sulfurized at 550 °C and 600 °C. From these spectra, the peaks corresponding to crystal planes of (112), (204), and (312) (PDF 44-1476) can be observed, which indicate the stannite structure for CFTS material. At first glance, we can see that no index peak is evident at 600 °C, but for the sample sulfurized at 550 °C, there is an index peak at the angle of 28.39°, which is related to the crystal plan of (112). The suppression of this peak at 600 °C is because either the crystalline phase is not formed or the formed phase has a very weak peak that cannot be identified in the vicinity of the existing amorphous background. Therefore, examining the XRD pattern of this sample cannot provide a useful information. We emphasize that except for the sulfurization temperature, all other factors of production of the thin films were similar. Considering that the thin film is deposited on the glass substrate, the effects related to the substrate along with the secondary phases can also show themselves in the XRD pattern. This statement is realized by a relatively gentle elevation between angles of 10° and 40°. However, it does not damage the peak corresponding to the (112) plane.

One of the factors showing the improvement of the material quality in the XRD pattern is the significant peak's intensities. In other words, the higher the intensity of the peaks compared to the intensity of the background, the better the crystalline properties of the grown material.

According to the results deduced from Figure 1, we go ahead with the sulfurization at 550 °C to study the influence of laser fluence on the quality of the thin films. The surfaces of the produced samples are smooth and shiny but the 9.54 J/cm^2 sample includes some particulates on the surface, which may appear because of the high laser fluence.

Figure 2 represents the XRD patterns of the thin films deposited by different fluences and then sulfurized at 550 °C. By comparing the spectra of the samples grown by 3.82, 4.58 and 9.54 J/cm^2 fluences, we find that the intensity of (112) peak is higher for the 4.58 J/cm^2 sample, whereas a significant change is not felt in the spectra of the 3.82 J/cm^2 and 9.54 J/cm^2 samples. This means that the crystalline properties of the material are better formed by the fluence of 4.58 J/cm^2.

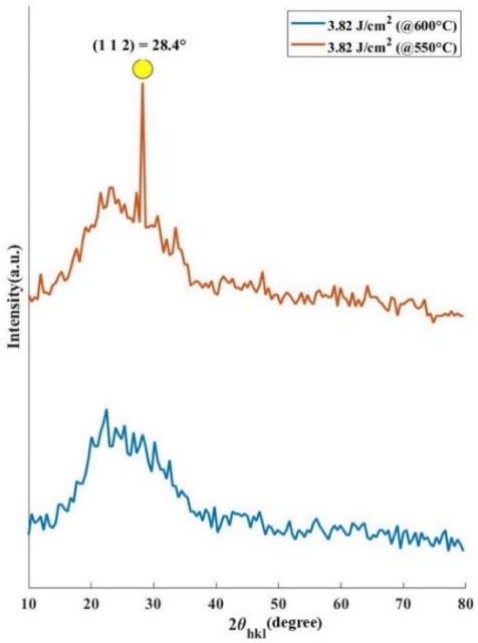

Fig. 1. XRD patterns for the CFTS layers produced by fluence of 3.82 J/cm2 and sulfurization at 600 and 550 °C.

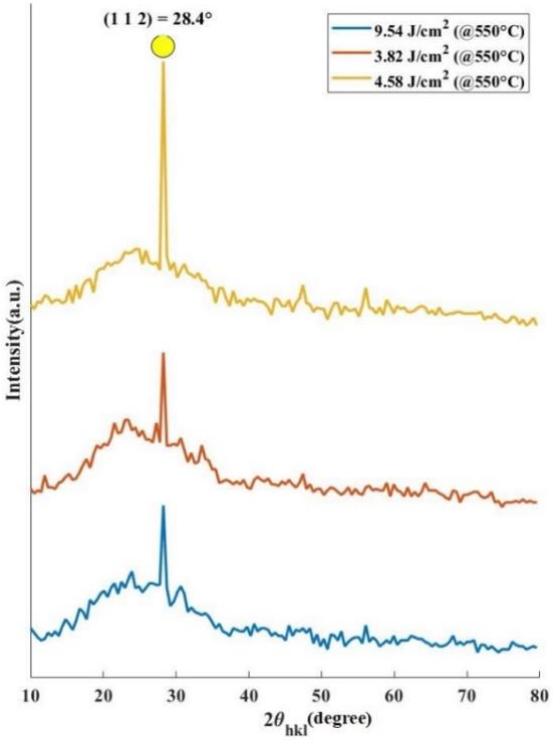

Fig. 2. XRD patterns for the CFTS layers produced by fluences of 3.82 J/cm2, 4.58 J/cm2 and 9.54 J/cm2, and sulfurization at 550 °C.

[Downloaded from mail.ijop.ir on 2026-11-26]

Table **1**. Crystal features of the samples

Sample	3.82 J/cm^2	4.58 J/cm^2	9.54 J/cm^2
Miller index	(112)	(112)	(112)
$2\theta_{hkl}$ (°)	28.4	28.4	28.4
β_{hkl} (°)	0.27	0.23	0.30
Crystallite size (nm)	33	38	24
Microstrain (%)	0.473	0.414	0.647
d_{hkl} (Å)	3.13	3.13	3.14
$\delta\left(10^{14}\ \frac{\text{Line}}{\text{m}^2}\right)$	11.1	7.3	17.36

Table **2**. Crystallographic parameters of the 4.58 J/cm^2 sample based on PDF-044-1476 and PDF-035-0582 cards

Parameter	PDF-044-1476	PDF-035-0582
a=b (Å)	5.4501	5.4531
C (Å)	10.739	10.747
α (°)	90	90
β (°)	90	90
γ (°)	90	90
V ($\times 10^6$ pm^3)	318.99	319.58
c/a	2	2

To verify this point, we compare the crystal characteristics of the samples in Table 1 by using equations (1- 4). As can be seen in this Table, the 28.4° peak does not show a sensible shift, but the corresponding β_{hkl} value of the samples has changed. According to equation (2), the smaller the amount of β_{hkl}, the larger crystallites in the material. The larger crystallite of the sample 4.58 J/cm^2, is accompanied with the lower lattice strain, which confirms the better crystal quality of the sample produced by the laser fluence of 4.58 J/cm^2. Lattice constants of the 4.58 J/cm^2 sample are represented in Table 2. The data is in accordance with PDF-044-1476 and PDF-035-0582 card numbers [9, 10]. The results are also in good coincidence with the data reported in literature [11-13]. The deviation is about 1%, which is completely normal.

Due to the similar XRD patterns of the samples it is necessary to study the Raman spectra of the samples for more information. Figure 3 shows the Raman spectra for the samples. More than 30 different peaks might be found in the Raman spectrum of CFTS material, which vary depending on the thin film growth process, structure, and material purity [5, 8, 10, 14]. The 311 cm^{-1} peak is common, which is the most intense peak in these three spectra. Moreover, the peaks of 275 cm^{-1}, 246 cm^{-1}, and 134 cm^{-1} in 3.82 J/cm^2 sample, and 279 cm^{-1} peak in 9.54 J/cm^2 one are also realized. Although the 311 cm^{-1} peak has been observed in all three spectra, the peak indicating the stannite structure for CFTS is 318 cm^{-1} peak [14].

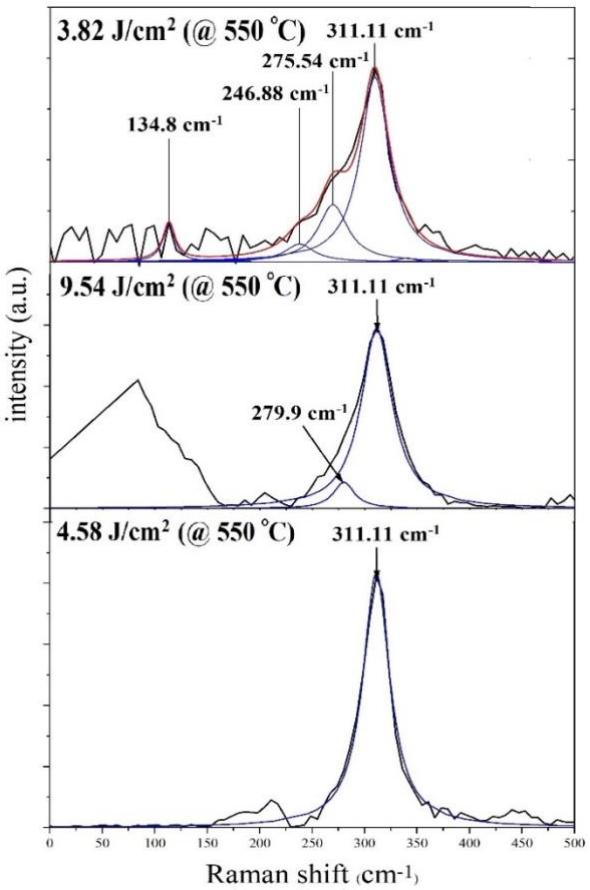

Fig. 3. Raman spectra of the CFTS structures sulfurized at 550 °C. The main Raman spectrum is shown with a black line, the Lorentz line fits the Raman spectrum with a red color, and the profiles forming the Lorentz line are shown with blue lines.

The main Raman peak of our samples shows a shift of about 7 cm^{-1} from the peak 318 cm^{-1}. Such a shift occurs for all other peaks in Raman spectra. The shift of the peaks in the Raman spectrum is not related to the presence of secondary phases such as Cu_2SnS_3 (290 cm^{-1}), CuS (474 cm^{-1}), etc., but it is because of sulfurization procedure. In fact, the vibrational levels of the molecules will change with the temperature rate in the sulfurization process. As a result, the bond length (molecule volume) changes accordingly. This causes the A_1 modes shift towards lower frequencies in the Raman

[Downloaded from mail.ijop.ir on 2026-11-26]

spectrum, which include just the motion of the anions [15-18]. Therefore, the obtained results show a shift around 7 cm^{-1} that is common considering the amount of temperature rate in the sulfurization process. Nevertheless, the features and accuracy of the employed spectrometer should not be overlooked. Eventually, regarding the presented statement, we can conclude that the Raman spectra in Figure 3 confirm the stannite structure of the deposited thin films.

The Raman spectra also provide more distinguish between the two samples, 3.82 J/cm^2 and 9.54 J/cm^2, whose XRD patterns are very similar. The main difference between these two samples is the presence of additional peaks, unrelated to the CFTS structure, in the frequency range of 0-150 cm^{-1} in the Raman spectrum of the 9.54 J/cm^2 sample. The existence of these extra peaks specifies an increase in the secondary phases' fraction in the 9.54 J/cm^2 sample compared to the other one. The larger portion of the secondary phases in the 9.54 J/cm^2 sample forms because of the higher laser fluence. When the more intense laser pulse hits the CFT tablet in the PLD process, the material can be torn as particulates from the target. The film deposited on the glass substrate also maintains this particulate structure. As a result, when the thin film is placed in the sulfurization process, the particulate structure cannot participate truly in the process of forming the crystal structure of CFTS. Therefore, the increase in of secondary phases is inevitable. It can be concluded that among these two samples, the 3.82 J/cm^2 one has better crystalline quality due to the lower fraction of secondary phases.

By analyzing the Raman spectra of 4.58 J/cm^2 and 3.82 J/cm^2 samples we can realize that the 311 cm^{-1} peak in the spectrum of the sample 4.58 J/cm^2 is more intense and thinner. This indicates that the type of molecular bonds in the 4.58 J/cm^2 sample is more uniform than that in the 3.82 J/cm^2 one [16, 17]. The Raman spectra can also provide qualitative information about the average grain size (GS). The FWHM size of the significant peak in the Raman spectrum has

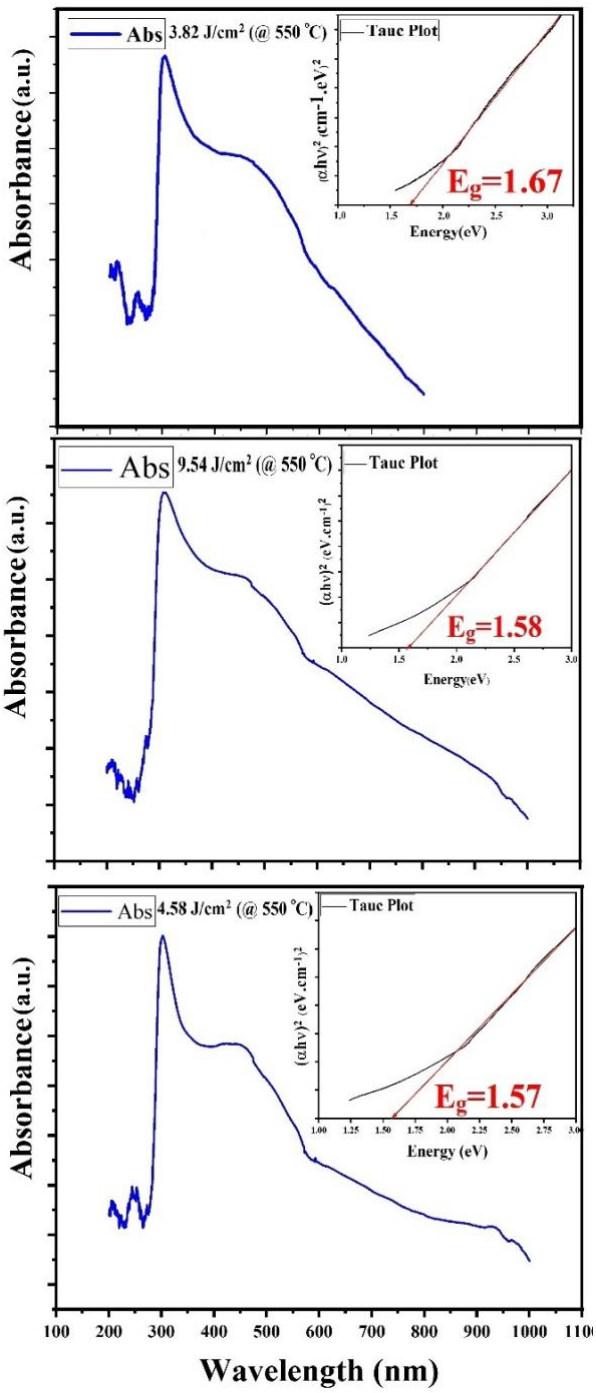

Fig. 4. UV-Vis-IR spectra of the CFTS thin films grown by PLD and sulfurized at 550 °C. The insets represent the corresponding Tauc plot.

a direct relationship with the grain size of each sample [19]. Regarding the FWHM of the Raman significant peak, it can be said that the order of grain size is as follows:

$$\mathrm{FWHM}_{4.58} < \mathrm{FWHM}_{3.82} < \mathrm{FWHM}_{9.54} \Rightarrow$$

$$\mathrm{GS}_{4.58} < \mathrm{GS}_{3.82} < \mathrm{GS}_{9.54}.$$

[Downloaded from mail.ijop.ir on 2026-11-26]

This finding is in accordance with the XRD results and means the improvement of the crystal quality of the material.

Figure 4 shows the UV-Vis-IR spectra of the thin films sulfurized at the temperature of 550 °C. These spectra which are in agreement with previous studies [20], demonstrate that the CFTS thin films, deposited by PLD method, have the highest absorption in a range around 305 nm. By analyzing the data and drawing the Tauc-plot (the insets), it is clear that the band gaps of the 3.82 J/cm^2, 9.54 J/cm^2, and 4.58 J/cm^2 samples are 1.67, 1.58 and 1.57 eV, respectively. As is seen, the difference is not significant and justifiable. It can also be seen that the absorption level of the material in 4.58 J/cm^2 is slightly reduced compared to the other samples due to the improvement of the crystalline state of the material.

V. CONCLUSION

We produced the CFT thin films by the PLD method, with fluences of 3.82, 4.58 and 9.54 J/cm^2, and then sulfurized them at temperatures of 550 °C and 600 °C to turn them into CFTS thin films. The analysis of the produced thin films indicated that the sulfurization of the metal thin film, carried out in a vacuum chamber after the PLD process, is well able to provide the CFTS structure. Moreover, according to the XRD and Raman spectra, it was found that with decreasing the sulfurization temperature from 600 °C to 550 °C, the likelihood of formation of CFTS phase increases and the resulting structure will find the stannite phase. We also investigated the influence of the laser fluence in the PLD process on the created thin films. Analyzing the samples by Raman spectroscopy showed that a proper excitation of CFT atoms in the PLD process can improve the quality of the thin films. This suitable excitation occurred at the fluence of 4.58 J/cm^2.

REFERENCES

[1] B. Saparov, "Next Generation Thin-Film Solar Absorbers Based on Chalcogenides," Chem. Rev., Vol. 122, pp. 10575-10577, 2022.

[2] T.K. Todorov, O. Gunawan, T. Gokmen, and B.M. David, "Solution-processed $Cu(In,Ga)(S,Se)_2$ absorber yielding a 15.2% efficient solar cell," Prog. Photovolt: Research Appl., Vol. 21, pp. 82-87, 2013.

[3] B. Ananthoju, J. Mohapatra, M.K. Jangid, D. Bahadur, N.V. Medhekar, and M. Aslam. "Cation/anion substitution in Cu_2ZnSnS_4 for improved photovoltaic performance," Sci. Rep., Vol. 6, pp. 1-11, 2016.

[4] G.L. Agawane, S.W. Shin, S.A. Vanalakar, A.V. Moholkar, and J.H. Kim, "Next generation promising $Cu_2(Zn_xFe_{1-x})SnS_4$ photovoltaic absorber material prepared by pulsed laser deposition technique," Mater. Lett., Vol. 137, pp. 147-149, 2014.

[5] S.A. Vanalakar, P.S. Patil, and J.H. Kim, "Recent advances in synthesis of Cu_2FeSnS_4 materials for solar cell applications: a review," Sol. Energy Materials Sol. Cells, Vol. 182, pp. 204-219, 2018.

[6] H. He, M. Xiao, Q. Zhong, Y.C. Fu, X.M. Shen, and J.M. Zeng, "Influence of laser pulse energy on the microstructure and optical properties of Cu_2ZnSnS_4 films by one-step pulsed laser deposition," Ceram. Int., Vol. 40, pp. 13263-13267, 2014.

[7] J.G. Hu, W. Tong, I. Muhammad, U. Farooq, S. Chen, Z.H. Zheng, Z.H. Su, X.D. Lin, P. Fan, H.L. Ma, and X.H. Zha, "Pulsed laser deposited and sulfurized Cu_2ZnSnS_4 thin film for efficient solar cell," Sol. Energy Mater. Sol. Cells, Vol. 233, pp. 111383 (1-8), 2021.

[8] E.G Fidha, N. Bitri, S. Mahjoubi, M. Abaab, and I. Ly, "Effect of the spraying temperatures and the sulfurization on the properties of the absorber Cu_2FeSnS_4 thin films in a solar cell," Mater. Lett., Vol. 215, pp. 62-64, 2018.

[9] A. Sugaki, A. Kitakaze, and K. Hayashi, "Synthesis of minerals in the Cu—Fe—Bi—S system under hydrothermal condition and their phase relations," Bull. de Minéralogie, Vol. 104, pp. 484-495, 1981.

[10] S.S. Pollack, G.J. McCarthy, and J.M. Holzer, "An Application of Calculated X-Ray Diffraction Patterns in the Analysis of Reference Powder Data: Trivalent Metal Sulfates," Powder Diffraction, Vol. 7, pp. 215-218, 1992.

[11] T. Shibuya, Y. Goto, Y. Kamihara, M. Matoba, K. Yasuoka, L.A. Burton, and A. Walsh, "From

[Downloaded from mail.ijop.ir on 2026-11-26]

kesterite to stannite photovoltaics: Stability and band gaps of the $Cu_2(Zn,Fe)SnS_4$ alloy," Appl. Phys. Lett., Vol. 104, pp. 021912-021915, 2014.

[12] X. Meng, H. Deng, J. Tao, H. Cao, X. Li, L. Sun, P. Yang, and J. Chu, "Heating rate tuning in structure, morphology and electricity properties of Cu_2FeSnS_4 thin films prepared by sulfurization of metallic precursors," J. Alloys Comp., Vol. 680, pp. 446-451, 2016.

[13] A. El Kissani, A. Abali, S. Drissi, L. Nkhaili, K. El Assail, A. Outzourhit, D.A. El Haj, and H. Chaib, "Earth Abundant Cu_2FeSnS_4 Thin Film Solar Cells," In 2021 9th International Renewable and Sustainable Energy Conference (IRSEC), IEEE, pp. 1-4, 2021.

[14] S. Wang, R.X. Ma, C.Y. Wang, S.N. Li, and H. Wang, "Effects of K ions doping on the structure, morphology and optical properties of Cu_2FeSnS_4 thin films prepared by blade-coating process," Optoelectron. Lett., Vol. 13, pp. 291-294, 2017.

[15] A.M. Abdulaziz, F. Alam, A. Salhi, M. Missous, A.G. Thomas, P. O'Brien, and D.J. Lewis, "A molecular precursor route to quaternary chalcogenide CFTS (Cu_2FeSnS_4) powders as potential solar absorber materials," RSC Adv., Vol. 9, pp. 24146-24153, 2019.

[16] S.P. Madhusudanan, M.S. Kumar, K. Mohanta, and S.K. Batabyal, "Photoactive Cu_2FeSnS_4 thin films: Influence of stabilizers," Appl. Surf. Sci., Vol. 535, pp. 147600 (1-8), 2021.

[17] C. Nefzi, M. Souli, J.L. Costa-Krämer, J.M. García, and N. Kamoun-Turki, "Growth of the next generation promising $Cu_2Fe_{1-x}Co_xSnS_4$ thin films and efficient p-CCTS/n-In_2S_3/n-SnO2F heterojunction for optoelectronic applications," Mater. Res. Bull., Vol. 133, pp. 111028 (1-9), 2021.

[18] I.M. El Radaf, H.Y.S. Al-Zahrani, S.S. Fouad, and M.S. El-Bana, "Profound optical analysis for novel amorphous Cu_2FeSnS_4 thin films as an absorber layer for thin film solar cells," Ceram. Int., Vol. 46, pp. 18778-18784, 2020.

[19] Y. Shen, N. Xu, J. Lai, J. Sun, J. Wu, Z. Ying, and T. Okada, "Fabrication of ZnO nanorods by pulsed Nd:YAG laser ablation deposition," J. Vac. Sci. Technol. B, Vol. 27, pp. 1856-1860, 2017.

[20] B. Ananthoju, J. Mohapatra, M.K. Jangid, D. Bahadur, N.V. Medhekar, and M. Aslam, "Cation/Anion Substitution in Cu_2ZnSnS_4 for Improved Photovoltaic Performance," Sci. Rep., Vol. 6, pp. 1-11, 2017.



Iman Rahmani was born in Kashmar in 1996. He received his B.Sc. degree in optics and laser engineering from Malek Ashtar University of Technology (MUT), Shahin Shar, Isfahan, Iran in 2019 and his M.Sc. degree in photonics from Shahid Beheshti University, Tehran, Iran in 2022. His research interests include thin films and pulsed laser deposition (PLD).



Majid Ghanaatshoar received his B.Sc. degree in physics from Isfahan University of Technology, Isfahan, Iran in 1992, the M.Sc. degree from Tehran University, Tehran, Iran in 1995 and his Ph.D. degree in condensed matter physics from Shahid Beheshti University, Tehran, Iran in 2002.

He is currently engaged as a professor of physics in Laser and Plasma Research Institute, Shahid Beheshti University, Tehran, Iran. His research interests span solar cells, nano photonics, plasmonics, optoelectronics, nano magnetism, magnetic semiconductors, and photonic bandgap materials.

[Downloaded from mail.ijop.ir on 2026-11-26]

THIS PAGE IS INTENTIONALLY LEFT BLANK.

[Downloaded from mail.ijop.ir on 2026-11-26]